Acta Cryst. (1998). B**54**, 732–740

Distribution of the *M*—*M* Distances in the Rare Earth Oxides

A. Vegas* and R. Isea†

Instituto de Química-Física 'Rocasolano', CSIC, Serrano 119, E-28006 Madrid, Spain. E-mail: xangel@roca.csic.es

(*Received 6 October 1997; accepted 4 March 1998*)

Abstract

A systematic study of the distribution of the *M*—*M* distances in all the binary, ternary and quaternary oxides of the rare earth elements (RE = Sc, Y, La–Lu), contained in the Inorganic Crystal Structure Database (ICSD) has been carried out. The results indicate that the RE—RE distances are not distributed uniformly, but present maxima which are close to the corresponding distances in the pure metals. In some of the histograms (Y, Ce, Pr, Sm, Tb, Dy, Ho, Lu) two maxima appear which correspond to the nearest-neighbor (b.c.c., h.c.p.) and second-nearest neighbor (b.c.c.) distances of the elemental phases. As examples of this behavior, the cation arrays of the binary oxides, hydroxides and ternary oxides of both the delafossite and α-$NaFeO_2$ type are analyzed. In all of them the cations form aggregates whose topologies and distances can be related to the structure of the parent metals. The size of the metal aggregates seems to decrease with increasing oxygen content.

1. Introduction

In two previous papers we have reported on the distribution of the *M*—*M* distances in all the Mg-, Ca- and Sr-containing compounds (Isea & Vegas, 1995) and in the binary, ternary and quaternary oxides of the Group 13 elements (Isea *et al.*, 1998). In all cases the *M*—*M* distances are not distributed uniformly, but the distribution functions present maxima coincident with the values of the *M*—*M* distances in the pure elements. These features seem to reflect a general trend in inorganic solids: the structures of the elements (topology and distances) are maintained in the compounds. We have given several examples of this (Vegas *et al.*, 1990, 1991; Vegas & Martínez-Ripoll, 1992; Vegas *et al.*, 1995; Ramos-Gallardo & Vegas, 1995, 1996).

In this paper we report a similar study of the distribution of the *M*—*M* distances in all the rare earth oxides (binary, ternary and quaternary) to see whether this behavior can be extended to these elements (RE = Sc, Y, La–Lu). The study is completed by an analysis of the topology and distances of the cation array in binary rare earth oxides, trihydroxides and the ternary oxides with both the delafossite- and α-$NaFeO_2$-type structures. Although this behavior was reported for *C*-Ln_2O_3 (Ramos-Gallardo & Vegas, 1995), it will be treated in more detail here. The oxyhydroxides have been examined previously (Vegas & Isea, 1997). In all of them the rare earth cations form more or less extended aggregates which can be related to the structure of the parent metals.

2. Data processing

The data for all the binary, ternary and quaternary oxides were obtained from the ICSD (Kirschhoff *et al.*, 1995), and further processed with the aid of a program (*BICSD*) written in TurboPascal7.0 for this purpose. It runs on a PC compatible with at least 1 Mb RAM. The data were reduced to obtain a set of unique entries. *M*—*M* distances for each compound were computed up to a value of 4.5 Å. This data reduction process was carried out using the criteria given elsewhere (Isea & Vegas, 1995; Isea *et al.*, 1998).

The number of unique entries and the number of computed distances for each compound are collected in Table 1. The final results are the histograms represented in Fig. 1, which contain the number of distances *N* at each interval of *d* (0.1 Å).

3. Results and discussion

As seen in Fig. 1, the histograms, far from being uniform, present maxima which are between the nearest-neighbor and second-nearest neighbor distances of the elemental phases, which are collected in Table 2. In the histograms of Y, Ce, Pr, Sm, Tb, Dy, Ho and Lu two maxima appear. The higher is close to the value of the shortest *M*—*M* distance in the f.c.c., h.c.p., La-type and b.c.c. metallic phases (d and $d_{\rm b.c.c.}$ in Table 2) and the lower one is close to the second-nearest neighbor distance of the elements. This last value corresponds to the unit-cell parameter of the b.c.c. metallic phase ($a_{\rm b.c.c.}$ in Table 2). For the remaining elements (La, Nd, Gd, Er and Tm) the histograms present a unique and wider maximum located between the extreme values cited above ($d_{\rm b.c.c.}$ and $a_{\rm b.c.c.}$). Only in the case of Sc, which has no b.c.c. phase, does the histogram present a unique and

---

† Permanent address: Centro de Química, IVIC, Apartado 21827, Caracas 1020A, Venezuela.

Table 1. *Number of compounds and number of computed* $M-M$ *distances up to 4.5 Å*

	Sc	Y	La	Ce	Pr	Nd	Sm	Eu	Gd	Tb	Dy	Ho	Er	Tm	Yb	Lu
No. of compounds	78	147	275	78	88	182	76	70	83	48	48	58	77	38	82	43
No. of distances	310	1134	1856	424	506	986	447	492	489	257	221	292	395	210	377	207

sharp maximum, which corresponds to the Sc—Sc distance in f.c.c.-Sc (3.21 Å) and is only 3% shorter than the same distance in h.c.p.-Sc (3.31 Å). Eu and Yb merit a special comment. These two elements are an exception in the sense that they have unit cells which are expanded with respect to the other lanthanides. The reason for this is the half-filled and filled *f* shell of Eu and Yb, respectively. However, when forming compounds they behave like the other elements giving rise to similar $M-M$ distances. Only Yb presents a high-pressure phase (b.c.c.), which is similar to the other lanthanides (see Table 2) and whose $d_{\mathrm{b.c.c.}}$ value (3.48 Å) corresponds to the first maximum in the histogram.

It is clear that when forming a compound, and owing to electronic and/or size effects, the metallic nets can undergo distortions giving rise to cation–cation distances which are close, but not exactly equal, to the $M-M$ distances in the pure metals. An example of this situation is the lanthanide oxyhydroxides (Vegas & Isea, 1997): their cation array can be described as a distorted fragment of a b.c.c. net in which the square (100) face has become rectangular, but where Σ, the sum of all the distances involved in the fragments, remains almost identical to the sum of the distances in the corresponding fragments of the elemental structures. These distortions could explain the appearance of a single and broad maximum in the histograms of La, Nd, Gd, Er and Tm. We have assumed that contractions and/or elongations of 4% in the $M-M$ distances could be taken as reasonable distortions and that, under these conditions, the majority of the $M-M$ distances in the histograms can be explained in terms of the $M-M$ distances of the pure metals. These distances correspond to the shaded areas in the histograms (Fig. 1). This area covers the whole maximum of Sc and a variable area of the remaining histograms, going from 65% in that of Nd up to 85% in the case of Y or even higher values in the case of Ho, Tm and Lu. To account for all the distances contained in the maxima, deviations up to 7% must be taken into account.

4. Description of the structures

4.1. *The rare earth sesquioxides*

The sesquioxides present three crystalline phases: (*a*) the cubic bixbyite-type C-Ln_2O_3, (*b*) the hexagonal A-Ln_2O_3 and (*c*) the monoclinic phase.

The cation array of the C-Ln_2O_3 phase has been described previously (Ramos-Gallardo & Vegas, 1995) and the $M-M$ distances were given for the Sc, Y, In and Tl compounds. As reported there, this structure is cubic, $Ia\bar{3}$, with the metal atoms at two different sites. The structure is related to that of fluorite in which 1/4 of the anions are missing and the MX_8 cubes of the fluorite structure become MX_6 distorted octahedra in the C-type structure. Distortion of the anion array also induces a distortion of the f.c.c. cation array of the CaF_2-type structure, giving rise to a three-dimensional network of centered M_7 hexagons, centered by $M(1)$ atoms. The structures of the sesquioxides of Y, Dy, Ho, Er, Tm and Yb (Faucher, 1980; Hase, 1963; Fert, 1962) have been refined in the centrosymmetric $Ia\bar{3}$ space group. Those of Sm, Eu, Gd, Tb and Lu (Zav'yalova *et al.*, 1976; Zachariasen, 1927) have been refined in the non-centrosymmetric $I2_13$ space group. All the interatomic distances for all these compounds are collected in Table 3. Although the accuracy attained in all the reported refinements is not uniform, the shortest $M-M$ distances and the second-nearest neighbor distances (around 4.00 Å) compare quite well with the corresponding values in the pure metals (see Table 2).

The monoclinic phases have been reported for Ln_2O_3, Ln = Sm, Eu, Tb (Schleid & Meyer, 1989; Yakel, 1979; Hubert-Paletta & Müller-Buschbaum, 1968). They crystallize in the space group $C2/m$ with unit-cell parameters for Sm_2O_3 of a = 14.9975, b = 3.6273, c = 8.8561 Å, β = 99.98°. The cation array is represented in Fig. 2. It can be described as a distortion of an La-type array in which some of the distances are shortened to values of 3.35, 3.31 and 3.28 Å for Sm, Eu and Tb, respectively, whereas others are elongated to values greater than 3.80 Å. This distorted h.c.p. array can be recognized in Fig. 2 (contacts longer than 3.80 Å have not been drawn). The mean values for the $M-M$ distances up to 3.80 Å are 3.72, 3.70 and 3.65 Å for Sm, Eu and Tb, respectively, and agree within 2% with the $M-M$ distances of h.c.p. Sm and h.c.p. Tb listed in Table 2. The anomalous behavior of Eu should be recalled.

The so-called hexagonal A-type phases have been reported for Ln_2O_3, Ln = La, Ce, Pr, Nd (Boucherle, 1975; Wolf & Hoppe, 1985). The prototype is La_2O_3 and a complete description of the structure can be found in the article by O'Keeffe & Hyde (1985). It is trigonal, $P\bar{3}m$, with a = 3.938, c = 6.136 Å and the La atoms at (1/3, 2/3, 0.2467). The cation array can also be described as a distorted h.c.p. structure in which the sequence *ABAB*... of the 3^6 layers is maintained in the oxides. Within a layer, the Ln atoms are separated at distances of 6 × 3.938, 6 × 3.891, 6 × 3.858 and 6 × 3.831 Å for

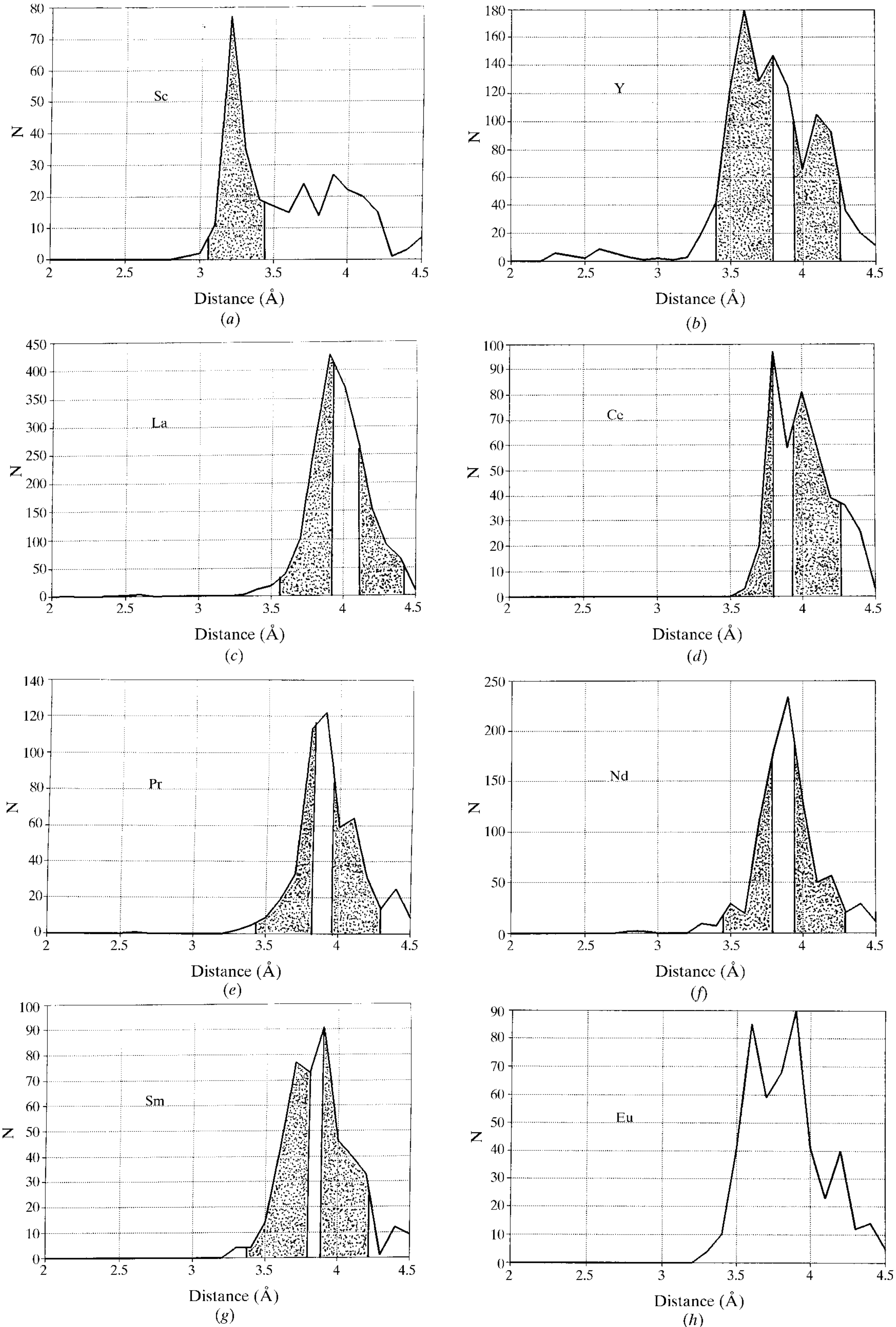

(a) (b) (c) (d) (e) (f) (g) (h)

Fig. 1. (*a*)–(*p*) Histograms showing the distribution of the *M*—*M* distances in all the binary, ternary and quaternary oxides of Sc, Y and Ln. The width of the intervals is 0.1 Å. The shaded area corresponds to the number of distances which deviate by ±4% from the values in the pure metals. The histograms of Eu and Yb, which present anomalies in the elemental state, are not shaded. In the case of Yb, the first maximum (3.50 Å) coincides exactly with the shortest Yb—Yb distance in the high-pressure phase (b.c.c.) of elemental Yb (3.48 Å).

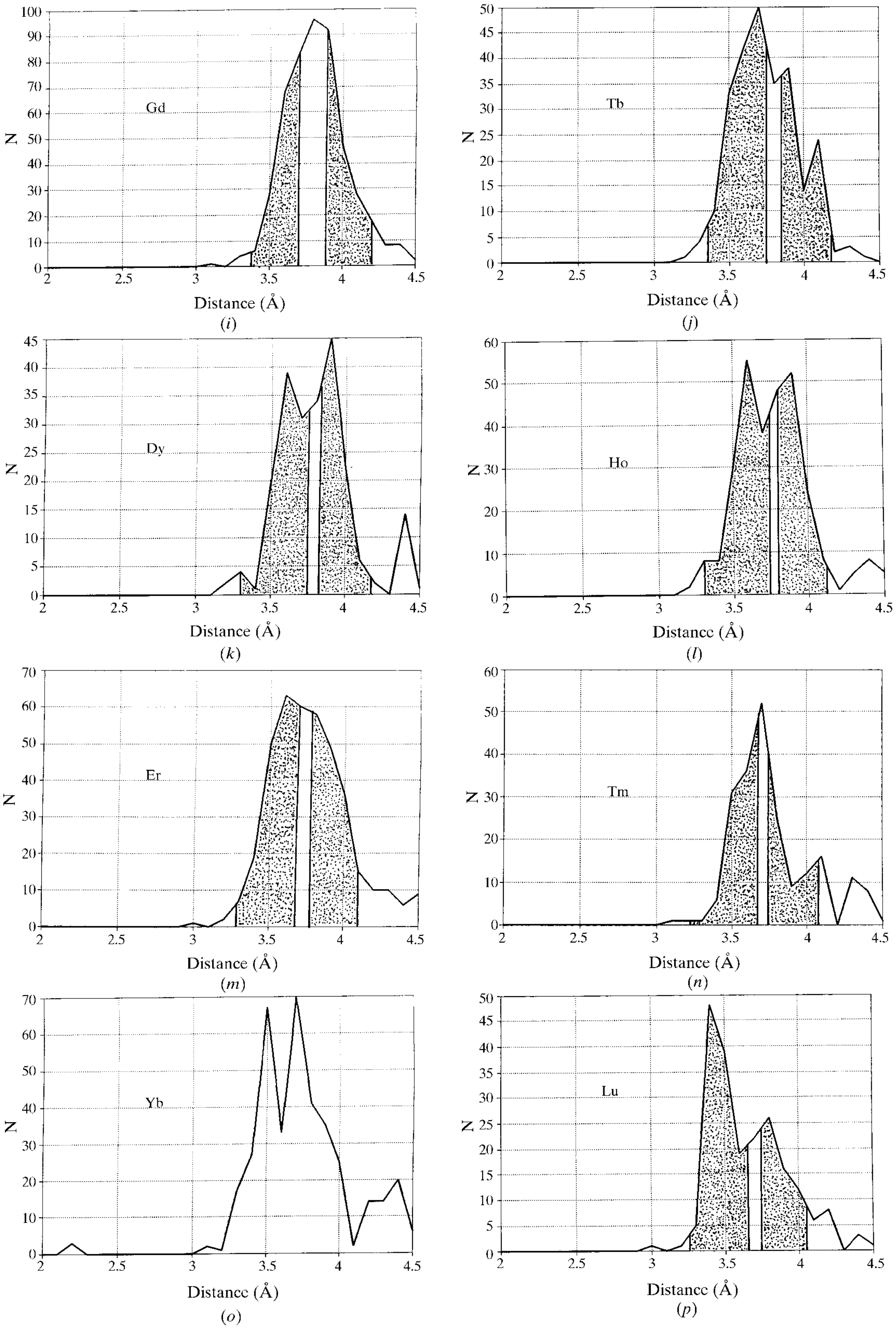
Gd
N
Distance (Å)
(i)
Tb
N
Distance (Å)
(j)
Dy
N
Distance (Å)
(k)
Ho
N
Distance (Å)
(l)
Er
N
Distance (Å)
(m)
Tm
N
Distance (Å)
(n)
Yb
N
Distance (Å)
(o)
Lu
N
Distance (Å)
(p)
2
2.5
3
3.5
4
4.5

Fig. 1. (*cont.*)

Table 2. *M—M distances in the elemental phases of the rare earths*

The *d* values are the shortest *M—M* distances in the f.c.c.-, h.c.p.- and La-type phases. $d_{\text{b.c.c.}}$ are the shortest *M—M* distances in the b.c.c. phases. $a_{\text{b.c.c.}}$ are the unit-cell parameters of the b.c.c. phases which are also the second-nearest neighbor distances.

RE	d	$d_{\text{b.c.c.}}$	$a_{\text{b.c.c.}}$
Sc	3.21†		
Sc	3.31‡		
Y	3.65‡	3.56	4.11
La	3.77§	3.69	4.26
Ce	3.65†	3.57	4.12
Pr	3.67§	3.58	4.13
Nd	3.65§	3.58	4.13
Sm	3.65‡	3.52	4.07
Eu	3.24†	3.97	4.58
Gd	3.56‡	3.51	4.05
Tb	3.60‡	3.48	4.02
Dy	3.59‡	3.45	3.98
Ho	3.58‡	3.43	3.96
Er	3.56‡	3.41	3.94
Tm	3.54‡	3.40	3.92
Yb¶	3.91‡	3.85	4.44
Lu	3.50‡	3.38	3.90

† f.c.c.-type. ‡ h.c.p.-type. § La-type. ¶ Yb has an additional high-pressure phase (b.c.c.) with $a = 4.02$, $d = 3.48$ Å. Note that this last value coincides with the first peak appearing in the histogram of Fig. 1.

La, Ce, Pr and Nd, respectively. These values correspond to the *a* parameter of the unit cell and are expanded by 5% with respect to the *M—M* distances in the elements (see Table 2). However, the six additional contacts with atoms of the upper and lower layers are closer to the values of the elemental structures. These contacts are 3 × 3.786 and 3 × 3.851 Å for La, 3 × 3.727 and 3 × 3.816 Å for Ce, 3 × 3.693 and 3 × 3.790 Å for Pr and 3 × 3.690 and 3 × 3.763 Å for Nd (*cf.* Table 2). Another interesting feature is that the spacing between two alternate layers (the *c* axis) almost coincides with the *c* axis of the corresponding metallic phases. In the oxides, these values are 6.14, 6.06, 6.01 and 6.00 Å for La, Ce, Pr and Nd, respectively. These spacings in the elemental structures have values of 6.08, 5.96, 5.92 and 5.90 Å, respectively. The deviations are less than 2%. In the case of Ce, which has neither the h.c.p.- nor the La-type structure, the latter value corresponds to the spacing between two alternate (111) layers in the f.c.c. structure.

4.2. *The rare earth dioxides*

For the rare earth dioxides two crystalline phases are known. CeO_2, PrO_2 and TbO_2 crystallize in the fluorite-type structure ($Fm\bar{3}m$) with unit-cell parameters of 5.389, 5.372 and 5.213 Å, respectively (Brauer & Gradinger, 1954; Grün *et al.*, 1951), and shortest *M—M* distances of 3.81, 3.80 and 3.69 Å, respectively. These values compare well (within 4%) with those listed in Table 2 for the elemental phases of Ce, Pr and Tb. It is well known that the cation array in the fluorite-type structures is f.c.c. with the anions inserted in all the tetrahedral holes. Thus, CeO_2 can be considered as the f.c.c.-Ce structure stuffed with O atoms, with an expansion of only 4% in the *M—M* distances. In the case of PrO_2, the f.c.c. fragments present in the La-type structure of Pr are stabilized in the oxide with an expansion of only 3.5% in the *M—M* distances. Finally, in TbO_2 the h.c.p. structure of metallic Tb is converted into the f.c.c. array of the oxide with an expansion of only 2.5% in the *M—M* distances. Insertion of two O atoms per Tb atom is accompanied by a volume increase of only 7.4%. It should be recalled that the insertion of two F atoms per Ca atom, in CaF_2 itself, takes place with a volume decrease of 6.6% in the f.c.c. structure of elemental calcium (O'Keeffe & Hyde, 1985) and that the three O atoms of some ABO_3 perovskites are inserted into the holes of the corresponding *AB* alloys without any volume increase (Martínez-Cruz *et al.*, 1994; Ramos-Gallardo & Vegas, 1997). Other compounds which behave in this manner are the tetragonal YbOOH (Vegas & Isea, 1997) and Cs_3BiO_3 (Zoche & Jansen, 1997).

The other crystalline phase known for RE dioxides has been reported for GdO_2 and EuO_2 (Imamov *et al.*, 1974), although structural data have only been given for GdO_2. It is tetragonal, *P*4/*nmm*, with $a = 3.94$, $c = 6.76$ Å and the Gd atoms at (0, 1/2, 0.182). The cation array is represented in Fig. 3. It consists of pairs of square 4^4 nets ($a = 3.94$ Å), perpendicular to *c*, shifted by (1/2, 1/2, 0) with respect to each other, in such a way that each Gd atom connects to another four of the contiguous layer at distances of 3.72 Å. This array is a fragment of a b.c.c. structure in which each (100) face and the body-centering atom [(200) plane] remain bonded, but the bonds between the latter and the $(\bar{1}00)$ faces are broken, producing the fragments which are separated by the inclusion of the oxygens. The similarity to the b.c.c. structure of elemental Gd is made evident when the Gd—Gd distances in b.c.c. Gd are compared with those in the oxide. Thus, the distance *d* (3.72 Å in the oxide) is expanded by ~6% with respect to the same distance in b.c.c. Gd (3.51 Å), whereas the *a* value (3.94 Å in the oxide) is contracted by 3% with respect to the unit-cell parameter of elemental Gd (4.05 Å). The expansion of *d*

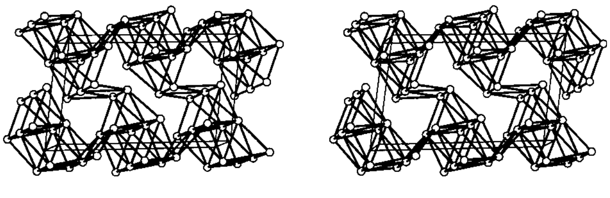

Fig. 2. Stereopair showing the cation array in the monoclinic phase of Sm_2O_3 to show its similarity with an La-type array. Atoms are bonded up to a distance of 3.8 Å.

Table 3. *M—M distances (Å) in the C-type rare earth sesquioxides*

In the compounds refined in the non-centrosymmetric $I2_13$ space group, the distances given are the mean values of all the similar distances around the three independent metal atoms.

Compound	Space group	$M(1)-M(2)$ $M(2)-M(2)$	Second-nearest neighbors	Reference
Y_2O_3	$Ia\bar{3}$	3.52 × 6 3.53 × 4	4.00	Faucher (1980)
Dy_2O_3	$Ia\bar{3}$	3.57 × 6 3.58 × 4	3.99	Hase (1963)
Ho_2O_3	$Ia\bar{3}$	3.54 × 6 3.56 × 4	3.95	Fert (1962)
Er_2O_3	$Ia\bar{3}$	3.45 × 6 3.47 × 4	3.94	Fert (1962)
Tm_2O_3	$Ia\bar{3}$	3.47 × 6 3.49 × 4	3.96	Hase (1963)
Yb_2O_3	$Ia\bar{3}$	3.45 × 6 3.46 × 4	3.94	Fert (1962)
Sm_2O_3	$I2_13$	3.59	4.05	Zav'yalova *et al.* (1976)
Eu_2O_3	$I2_13$	3.63	4.10	Zachariasen (1927)
Gd_2O_3	$I2_13$	3.56	4.07	Zachariasen (1927)
Tb_2O_3	$I2_13$	3.55	4.03	Zachariasen (1927)
Lu_2O_3	$I2_13$	3.45	3.92	Zachariasen (1927)

is partially compensated by the contraction of a in such a way that $\Sigma = 4(a + d)$ is comparable in both the oxide (30.63 Å) and the element (30.24 Å), indicating that GdO_2 can be described as the b.c.c. Gd structure broken into fragments by the inclusion of the O atoms, but where the structure of the element can yet be recognized.

4.3. *The rare earth hydroxides*

Two crystalline phases have been reported for $RE(OH)_3$. The structures of $Sc(OH)_3$ and $Lu(OH)_3$ are an exception in the general trend of all the $RE(OH)_3$. They are cubic $Im\bar{3}$ (Schubert & Seitz, 1948; Beall, Mullica *et al.*, 1977), with the metal atoms at the $8c$ site (1/4, 1/4, 1/4). The cations form a primitive cubic subnet with dimensions d = 4.11 and 3.94 Å for Lu and Sc, respectively. These distances are far from the shortest $M—M$ distances in elemental Sc and Lu (see Table 2) and hence no structural relationship can be established between them. We will return later to this problem.

All the other RE hydroxides are isostructural. They are hexagonal, $P6_3/m$, with the metal atoms at $2c$ (1/3, 2/3, 1/4). The unit-cell parameters and the RE—RE distances are collected in Table 4. The cation array can be described as linear chains, parallel to **c**, in which the cations are separated at distances which coincide with the first-neighbor distances in the h.c.p.-RE phases (compare the values of Table 2 and Table 4). Each chain is surrounded by three other chains, which are displaced **c**/2 with respect to the central one, and form hexagonal tunnels where the OH groups are inserted. Each metal atom is thus coordinated to six others forming a trigonal prism, at contact distances of ~4.00 Å. These values are similar to the a parameters of the b.c.c. nets of the elements (*cf.* Table 2 and Table 4). Note that these distances correspond to the second maximum in some of the histograms of Fig. 1.

4.4. *The delafossite-type structures*

The $A(RE)O_2$ dioxides, with A = Ag, Cu, crystallize in the delafossite-type structure. They are collected in Table 5. They are hexagonal, $P6_3/mmc$, with the RE atoms at $2a$ (0,0,0) and the A atoms at $2c$ (1/3, 2/3, 1/4). The structure consists of double layers of closest-packed O atoms with the RE atoms occupying all the octahedral holes. These double layers are stacked, along **c**, in such a way that they produce a twofold coordination of oxygens around the monovalent A cations. Regarding the cation array, the structure can be described as formed by alternate closest-packed 3^6 layers of RE and A atoms with the O atoms inserted into the tetrahedral holes formed by three RE and one A atoms. Within the 3^6 layers, the metal atoms are separated at distances which coincide with the a parameter of the hexagonal cell (see Table 5). Comparing these values with the RE—RE distances in the pure metals (see Table 2), one

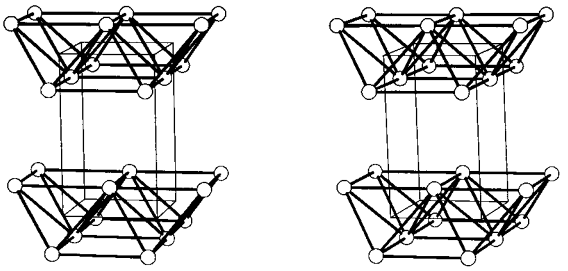

Fig. 3. Stereopair showing the Gd subnet in tetragonal GdO_2. The metallic fragments are formed by (100) and (200) planes of a b.c.c. structure, which has been broken by the inclusion of the O atoms.

Table 4. *Unit-cell parameters (Å) and M—M distances (Å) in the RE(OH)$_3$ hydroxides, crystallizing in the P6$_3$/m space group*

RE	*a*	*c*	*M—M* in the *ab* plane	Reference
Y	6.241	3.539	4.01 × 6	Christensen *et al.* (1967)
La	6.547	3.854	4.24 × 6	Beall, Milligan & Wolcott (1977)
Ce	6.489	3.806	4.20 × 6	Mullica, Oliver & Milligan (1979)
Pr	6.456	3.769	4.18 × 6	Mullica, Milligan & Beall (1979)
Nd	6.418	3.743	4.15 × 6	Beall *et al.* (1976)
Sm	6.368	3.683	4.11 × 6	Beall, Milligan & Wolcott (1977)
Gd	6.329	3.631	4.08 × 6	Beall, Milligan & Wolcott (1977)
Tb	6.308	3.600	4.06 × 6	Beall, Milligan, Korp & Bernal (1977)
Dy	6.286	3.577	4.05 × 6	Beall, Milligan & Wolcott (1977)
Ho	6.266	3.553	4.03 × 6	Beall, Milligan & Wolcott (1977)
Er	6.243	3.527	4.01 × 6	Beall, Milligan & Wolcott (1977)
Tm	6.221	3.503	4.00 × 6	Mullica, Milligan & Beall (1979)
Yb	6.216	3.474	3.99 × 6	Beall, Mullica *et al.* (1977)

can see that the RE atoms reproduce, in the delafossite structures, the values of the same distances in the pure elements. The largest deviation is observed for the Y compounds in which the Y—Y distances are 4% shorter than in h.c.p. Y (3.65 Å), but are much closer to the Y—Y distances in b.c.c. Y (3.56 Å). In all the other compounds the deviations are less than 2% (recall the anomaly observed in elemental Eu). Thus, this structure could also be regarded as the h.c.p.-RE structure in which the original 3^6 layers have been separated by the inclusion of linear CuO$_2$ or AgO$_2$ groups. Consequently, the Ag or the Cu subnets are expanded with respect to their elemental structures. The Ag—Ag and Cu—Cu distances are equal to the distances between the RE^{3+} cations.

4.5. *The α-NaFeO$_2$-type structures*

This type of structure is related to that of delafossite in the sense that it is also formed by double layers of closest-packed oxygens with the trivalent cations occupying all the octahedral holes. These double layers are not stacked as in the delafossite-type structure, but they produce c.c.p. anions in which the new octahedral holes are occupied by the monovalent cations. The structure can also be described as derived from the NaCl-type structure, in which cations of the same kind are grouped in sheets parallel to (111) producing a trigonal superstructure along [111]. These compounds are trigonal, $R\bar{3}m$, with the trivalent cations at 3*a* (0, 0, 0) and the monovalent cations at 3*b* (0, 0, 1/2). They are listed in Table 6 together with the shortest *M—M* distances, which are coincident with the *a* axis of the hexagonal *R* unit cell. Looking at these values and comparing them with those listed in Table 2, one can see that the 3^6 planar nets existing in f.c.c. Sc and h.c.p. RE are maintained in the oxides in such a way that the latter can be regarded as the original h.c.p. elemental structure expanded along **c** by the inclusion of the octahedral *M*O$_2$ layers containing the monovalent cations. The difference between both arrays is that the *ABAB*... sequence of h.c.p. RE is converted into the *ABCABC*... sequence of the oxides. Also in this case, the structure of the oxide can be described in terms of fragments of the elemental structure whose topology and distances are maintained in the oxides.

5. Conclusions

The results just discussed indicate that the features previously reported for rare earth oxyhydroxides (Vegas & Isea, 1997) are not isolated examples, but seem to obey a more general principle by which rare earth cations reproduce, in their compounds, both the topology and distances of the parent metal structure. This behavior is similar to that found in the alkaline earth metals (Isea & Vegas, 1995) and also in the elements of Group 13 (Isea *et al.*, 1998).

From the histograms represented in Fig. 1 it can be concluded that this feature affects not only first-neighbor distances (around 3.6 Å) but also the second-nearest neighbor distances, which correspond to the unit-cell parameter of the b.c.c. phases and which appear as a sharp maximum in some of the histograms of Fig. 1. Comparing these histograms with the values listed in Table 2 it can be concluded that the agreement is quite satisfactory. In all cases, except for Nd and Gd, the first maximum deviates by $\leq$ 3% from the shortest *M—M* distances in the pure elements.

It could be argued that what we are describing as metal aggregates are a mere consequence of the holes occupied by cations in close-packed arrays of O^{2-} anions. However, it should be recalled that similar distances also appear in (RE)B$_4$ and (RE)B$_6$ (Vegas *et al.*, 1995) and that these compounds are far from being considered in this manner.

The size of the metal aggregates seems to depend on the oxygen content. Thus, three-dimensional aggregates are observed in (RE)$_2$O$_3$ sesquioxides, two-dimensional clusters are present in the *A*(RE)O$_2$ dioxides and linear chains appear in the (RE)(OH)$_3$ hydroxides.

Table 5. *The A(RE)O$_2$ compounds crystallizing in the delafossite-type structure*

The values listed are the shortest RE—RE distances (× 6), which correspond to the *a* axes of the hexagonal unit cell of the respective oxide.

Compound	RE—RE distance (Å)	Reference
$CuScO_2$	3.22	Köhler & Jansen (1986)
$CuYO_2$	3.52	Köhler & Jansen (1986)
$CuLaO_2$	3.83	Haas & Kordes (1969)
$CuPrO_2$	3.75	Haas & Kordes (1969)
$CuNdO_2$	3.71	Haas & Kordes (1969)
$CuSmO_2$	3.66	Haas & Kordes (1969)
$CuEuO_2$	3.63	Haas & Kordes (1969)
$AgScO_2$	3.21	Shannon *et al.* (1971)
$AgYO_2$	3.50	Jansen (1996)

Table 6. *Compounds crystallizing in the α-NaFeO$_2$-type structure*

The RE—RE distances (× 6) coincide with the *a* axis of the hexagonal *R* cell.

Compound	RE—RE distance (Å)	Reference
$NaScO_2$	3.17	Hoppe *et al.* (1965)
$KScO_2$	3.22	Hoppe & Sabrowsky (1965)
$RbScO_2$	3.25	Wiench & Brachtel (1977)
KYO_2	3.46	Hoppe & Sabrowsky (1968)
$RbYO_2$	3.48	Hoppe & Sabrowsky (1968)
$CsYO_2$	3.52	Hoppe & Sabrowsky (1968)
$KLaO_2$	3.70	Clos *et al.* (1967)
$RbLaO_2$	3.74	Brunn & Hoppe (1975)
$KPrO_2$	3.64	Clos *et al.* (1970)
$RbNdO_2$	3.64	Brunn & Hoppe (1975)
$CsNdO_2$	3.67	Brunn & Hoppe (1975)
$RbSmO_2$	3.60	Brunn & Hoppe (1975)
$RbEuO_2$	3.57	Brunn & Hoppe (1975)
$RbGdO_2$	3.55	Brunn & Hoppe (1975)
$KErO_2$	3.43	Clos *et al.* (1967)

It is clear that the present features cannot be understood in the light of the ionic model. The appearance of Sc aggregates in Sc_2O_3 should be difficult to justify with a model which assumes the existence of Sc^{3+}, a cation with a noble gas configuration and incapable of forming Sc—Sc interactions. This led us to consider that electron transfer from Sc, Y or La to the oxygens could not be completely achieved and that part of the non-transferred electrons should be involved in *M*—*M* interactions. In support of this assumption are the *ab initio* calculations of second electron affinities of divalent anions carried out by Janoschek (1992). His conclusion is that anions such as O^{2-}, SO_4^{2-} *etc.* are unstable with respect to spontaneous ionization and that they must be designated as non-existent. Partial electron transfer is normally correlated with covalency in the sense that part of the metal states can be involved in the formation of directed *M*—O covalent bonds and where the *M* atoms are considered as isolated entities. This is especially true in the case of rare earths, where the inner *f* electrons should be unable to form *M*—*M* interactions. However, the features presented here show that the *M* atoms do not behave as isolated entities, but as fragments of the parent metal structure, indicating that some kind of interaction must exist between them. If not, how to explain the structures of the α-$NaFeO_2$ type in which both the RE atoms and the alkali atoms form separated 3^6 nets rather than being disordered and occupying statistically the octahedral holes of the f.c.c. O array?

The present results may also be correlated with those of a recent electron density study on Y_2O_3, Dy_2O_3 and Ho_2O_3 (Maslen *et al.*, 1996). The residual electron density around the metal atoms, far from being spherical, present maxima which are directed toward the six nearest metal atoms. Thus, the residual charge does not seem to be influenced by the pseudo-octahedral coordination of the O atoms, but by the cation geometry. This residual electron density near the RE cations has been interpreted as due to *d*–*f* exchange interactions. However, the appearance of similar maxima around the Y^{3+} cation, in Y_2O_3, with no *f* electron and with a noble gas configuration, is difficult to explain unless we admit a partial electron transfer from the metal to the O atoms. This reasoning, however, could not be applied to compounds such as $Y(OH)_3$ and $La(OH)_3$, in which complete electron transfer is, in principle, possible from Y and La to the OH groups and, nevertheless, linear chains of metal atoms exist in the compounds at distances similar to those of the pure metals. In our opinion, an electron density study on some of these hydroxides should be of great interest in order to establish whether features similar to those observed in the sesquioxides are also present in the linear chains of the hydroxides.

Finally, a comment should be made on $Sc(OH)_3$ and $Lu(OH)_3$. As mentioned above, these two compounds are an exception in the general behavior of the RE hydroxides. In the former, Sc and Lu atoms are hexacoordinated by six oxygens, whereas each oxygen is only coordinated by two metal atoms. However, in the other $(RE)(OH)_3$ compounds the cations are surrounded by nine oxygens and each O atom is coordinated by three cations. It is clear that this feature cannot be justified by size effects, scandium and lutetium being the smallest cations within this series, and there seems to be no reason for three Sc or Lu atoms to coordinate around each O atom. It is then possible that at high pressures, $Sc(OH)_3$ and $Lu(OH)_3$ could stabilize new phases, isostructural with the other $(RE)(OH)_3$ compounds, in which the coordination number around the cations could be increased from six to nine and consequently the coordination number around each anion could be increased from two to three. High-pressure experiments are being planned to check this assumption.

This work was supported by DGICYT (Spain) under project No. PB93-0118. One of us (RI) thanks the AECI (Spain) for financial support.

References

Beall, G. W., Milligan, W. O., Dillin, D., Williams, R. & McCoy, J. (1976). *Acta Cryst.* B**32**, 2227–2229.

Beall, G. W., Milligan, W. O., Korp, J. & Bernal, I. (1977). *Acta Cryst.* B**33**, 3134–3136.

Beall, G. W., Milligan, W. O. & Wolcott, H. A. (1977). *J. Inorg. Nucl. Chem.* **39**, 65–70.

Beall, G. W., Mullica, D. F., Milligan, W. O., Korp, J. & Bernal, I. (1977). *Inorg. Nucl. Chem. Lett.* **13**, 173–174.

Boucherle, J. X. (1975). *Acta Cryst.* B**31**, 2745–2746.

Brauer, G. & Gradinger, H. (1954). *Z. Anorg. Allg. Chem.* **417**, 89–95.

Brunn, H. & Hoppe, R. (1975). *Z. Anorg. Allg. Chem.* **417**, 213–220.

Christensen, A. N., Hazell, R. G. & Nilsson, A. (1967). *Acta Chem. Scand.* **21**, 481–492.

Clos, R., Devalette, M., Fouassier, C. & Hagenmuller, P. (1970). *Mater. Res. Bull.* **5**, 179–184.

Clos, R., Devalette, M., Hagenmuller, P., Hoppe, R. & Paletta, E. (1967). *C. R. Acad. Sci. Paris Ser. C*, **265**, 801–804.

Faucher, M. (1980). *Acta Cryst.* B**36**, 3209–3211.

Fert, A. (1962). *Bull. Soc. Fr. Cristallogr.* **85**, 267–270.

Grün, D. M., Köhler, W. C. & Katz, J. J. (1951). *J. Am. Chem. Soc.* **73**, 1475–1479.

Haas, H. & Kordes, E. (1969). *Z. Kristallogr.* **129**, 250–270.

Hase, W. (1963). *Phys. Status Solidi*, **3**, 446–449.

Hoppe, R. & Sabrowsky, H. (1965). *Z. Anorg. Allg. Chem.* **339**, 144–154.

Hoppe, R. & Sabrowsky, H. (1968). *Z. Anorg. Allg. Chem.* **357**, 202–214.

Hoppe, R., Schepers, B., Röhrborn, H. J. & Vielhaber, E. (1965). *Z. Anorg. Allg. Chem.* **339**, 130–143.

Hubert-Paletta, E. & Müller-Buschbaum, H. (1968). *Z. Anorg. Allg. Chem.* **363**, 145–150.

Imamov, R. M., Ragimly, N. A. & Semiletov, S. A. (1974). *Kristallografiya*, **19**, 751–753.

Isea, R. & Vegas, A. (1995). *C. R. Acad. Sci. Paris Ser. B*, **320**, 397–402.

Isea, R., Vegas, A. & Ramos-Gallardo, A. (1998). *Acta Cryst.* B**54**, 35–40.

Janoschek, R. (1992). *Z. Anorg. Allg. Chem.* **616**, 101–104.

Jansen, M. (1996). Private communication.

Kirschhoff, A., Pebler, A., Warkentin, E., Bergerhoff, G. & Luksch, P. (1995). ICSD. Fachinformationszentrum, Karlsruhe, Germany.

Köhler, B. U. & Jansen, M. (1986). *Z. Anorg. Allg. Chem.* **543**, 73–80.

Martínez-Cruz, L. A., Ramos-Gallardo, A. & Vegas, A. (1994). *J. Solid State Chem.* **110**, 397–398.

Maslen, E. N., Streltsov, V. A. & Ishizawa, N. (1996). *Acta Cryst.* B**52**, 414–422.

Mullica, D. F., Milligan, W. O. & Beall, G. W. (1979). *J. Inorg. Nucl. Chem.* **41**, 525–532.

Mullica, D. F., Oliver, J. D. & Milligan, W. O. (1979). *Acta Cryst.* B**35**, 2668–2670.

O'Keeffe, M. & Hyde, B. G. (1985). *Struct. Bonding (Berlin)*, **61**, 77–144.

Ramos-Gallardo, A. & Vegas, A. (1995). *J. Solid State Chem.* **119**, 131–133.

Ramos-Gallardo, A. & Vegas, A. (1996). *Z. Kristallogr.* **211**, 299–303.

Ramos-Gallardo, A. & Vegas, A. (1997). *J. Solid State Chem.* **128**, 69–72.

Schleid, T. & Meyer, G. (1989). *J. Less-Common Met.* **149**, 73–80.

Schubert, K. & Seitz, A. (1948). *Z. Anorg. Allg. Chem.* **256**, 226–238.

Shannon, R. D., Rogers, D. B. & Prewitt, C. T. (1971). *Inorg. Chem.* **10**, 713–718.

Vegas, A. & Isea, R. (1997). *J. Solid State Chem.* **131**, 358–362.

Vegas, A., Martínez-Cruz, L. A., Ramos-Gallardo, A. & Romero, A. (1995). *Z. Kristallogr.* **210**, 574–580.

Vegas, A. & Martínez-Ripoll, M. (1992). *Acta Cryst.* B**48**, 747–752.

Vegas, A., Romero, A. & Martínez-Ripoll, M. (1990). *J. Solid State Chem.* **88**, 594–596.

Vegas, A., Romero, A. & Martínez-Ripoll, M. (1991). *Acta Cryst.* B**47**, 17–23.

Wiench, H. & Brachtel, G. (1977). *Z. Anorg. Allg. Chem.* **436**, 169–172.

Wolf, R. & Hoppe, R. (1985). *Z. Anorg. Allg. Chem.* **529**, 61–64.

Yakel, H. L. (1979). *Acta Cryst.* B**35**, 564–569.

Zachariasen, W. (1927). *Nor. Geol. Tidsskr.* **9**, 310–316.

Zav'yalova, A. A., Imamov, R. M., Ragimly, N. A. & Semiletov, S. A. (1976). *Kristallografiya*, **21**, 727–729.

Zoche, N. & Jansen, M. (1997). *Z. Anorg. Allg. Chem.* **623**, 832–836.